

## NMR Spectroscopic Elucidation of the B–Z Transition of a DNA Double Helix Induced by the Z $\alpha$ Domain of Human ADAR1

Young-Min Kang,<sup>†</sup> Jongchul Bang,<sup>‡</sup> Eun-Hae Lee,<sup>†</sup> Hee-Chul Ahn,<sup>§</sup> Yeo-Jin Seo,<sup>†</sup> Kyeong Kyu Kim,<sup>||</sup> Yang-Gyun Kim,<sup>⊥</sup> Byong-Seok Choi,<sup>‡,\*</sup> and Joon-Hwa Lee<sup>†,\*</sup>

*Department of Chemistry, RINS, and Environmental Biotechnology National Core Research Center, Gyeongsang National University, Jinju, Gyeongnam 660-701, Korea, Department of Chemistry and National Creative Research Initiative Center, KAIST, Daejeon 305-701, Korea, Advanced Analysis Center, KIST, Seoul 130-650, Korea, Department of Molecular Cell Biology, Sungkyunkwan University School of Medicine, Suwon, Gyeonggi 440-746, Korea, and Department of Chemistry, Sungkyunkwan University, Suwon, Gyeonggi 440-746, Korea*

Received April 3, 2009

**Abstract:** The human RNA editing enzyme ADAR1 (double-stranded RNA deaminase I) deaminates adenine in pre-mRNA to yield inosine, which codes as guanine. ADAR1 has two left-handed Z-DNA binding domains, Z $\alpha$  and Z $\beta$ , at its NH<sub>2</sub>-terminus and preferentially binds Z-DNA, rather than B-DNA, with high binding affinity. The cocrystal structure of Z $\alpha$ <sub>ADAR1</sub> complexed to Z-DNA showed that one monomeric Z $\alpha$ <sub>ADAR1</sub> domain binds to one strand of double-stranded DNA and a second Z $\alpha$ <sub>ADAR1</sub> monomer binds to the opposite strand with 2-fold symmetry with respect to DNA helical axis. It remains unclear how Z $\alpha$ <sub>ADAR1</sub> protein specifically recognizes Z-DNA sequence in a sea of B-DNA to produce the stable Z $\alpha$ <sub>ADAR1</sub>–Z-DNA complex during the B–Z transition induced by Z $\alpha$ <sub>ADAR1</sub>. In order to characterize the molecular recognition of Z-DNA by Z $\alpha$ <sub>ADAR1</sub>, we performed circular dichroism (CD) and NMR experiments with complexes of Z $\alpha$ <sub>ADAR1</sub> bound to d(CGCGCG)<sub>2</sub> (referred to as CG6) produced at a variety of protein-to-DNA molar ratios. From this study, we identified the intermediate states of the CG6–Z $\alpha$ <sub>ADAR1</sub> complex and calculated their relative populations as a function of the Z $\alpha$ <sub>ADAR1</sub> concentration. These findings support an *active* B–Z transition mechanism in which the Z $\alpha$ <sub>ADAR1</sub> protein first binds to B-DNA and then converts it to left-handed Z-DNA, a conformation that is then stabilized by the additional binding of a second Z $\alpha$ <sub>ADAR1</sub> molecule.

### Introduction

Left-handed Z-DNA was first found in a polymer of alternating d(CG)<sub>n</sub> under high salt conditions,<sup>1</sup> and its structure was first reported in an X-ray crystallographic study.<sup>2</sup> In contrast to right-handed B-DNA, the Z-DNA helix is built from dinucleotide repeats with the dC in the anti conformation and the dG in the unusual syn conformation, which causes the backbone to follow a zigzag path.<sup>3,4</sup> Z-DNA is a higher energy conformation than B-DNA and is stabilized by negative supercoiling generated *in vivo*.<sup>3,4</sup> For example, negative supercoils arise behind a moving RNA polymerase during transcription and provide the energy for conversion from B-DNA to Z-DNA.<sup>5</sup>

Double-stranded RNA deaminase I (ADAR1) deaminates adenine in pre-mRNA to yield inosine (I), which codes as a guanine residue in mRNA.<sup>6</sup> These A → I conversions can lead to functional changes in the resulting proteins. For example, A → I conversions modulate the calcium permeability of neural glutamate receptors<sup>7</sup> and reduce the G-protein coupling efficacy of serotonin 2C receptors.<sup>8</sup> At its NH<sub>2</sub>-terminus, ADAR1 has two left-handed Z-DNA binding domains, Z $\alpha$  and Z $\beta$ .<sup>9</sup> Specific binding of the Z $\alpha$  domain of human ADAR1 (Z $\alpha$ <sub>ADAR1</sub>) to Z-DNA was shown originally by a band-shift assay<sup>10</sup> and later confirmed by circular dichroism (CD) and Raman spectroscopy.<sup>11,12</sup> The crystal structure of Z $\alpha$ <sub>ADAR1</sub> complexed to Z-DNA revealed

\* Corresponding authors: e-mail byongseok.choi@kaist.ac.kr (B.-S.C.) or joonhwa@gnu.ac.kr (J.-H.L.).

<sup>†</sup> Gyeongsang National University.

<sup>‡</sup> KAIST.

<sup>§</sup> KIST.

<sup>||</sup> Department of Molecular Cell Biology, Sungkyunkwan University School of Medicine.

<sup>⊥</sup> Department of Chemistry, Sungkyunkwan University.

- (1) Pohl, F. M.; Jovin, T. M. *J. Mol. Biol.* **1972**, *67*, 375–396.
- (2) Wang, A. H.; Quigley, G. J.; Kolpak, F. J.; Crawford, J. L.; van Boom, J. H.; van der Marel, G.; Rich, A. *Nature* **1979**, *282*, 680–686.
- (3) Herbert, A.; Rich, A. *J. Biol. Chem.* **1996**, *271*, 11595–11598.
- (4) Herbert, A.; Rich, A. *Genetica* **1999**, *106*, 37–47.
- (5) Liu, L. F.; Wang, J. C. *Proc. Natl. Acad. Sci. U.S.A.* **1987**, *84*, 7024–7027.

- (6) Schwartz, T.; Rould, M. A.; Lowenhaupt, K.; Herbert, A.; Rich, A. *Science* **1999**, *284*, 1841–1845.

- (7) Sommer, B.; Kohler, M.; Sprengel, R.; Seeburg, P. H. *Cell* **1991**, *67*, 11–19.

- (8) Burns, C. M.; Chu, H.; Rueter, S. M.; Hutchinson, L. K.; Canton, H.; Sanders-Bush, E.; Emeson, R. B. *Nature* **1997**, *387*, 303–308.

- (9) Schade, M.; Turner, C. J.; Kuhne, R.; Schmieder, P.; Lowenhaupt, K.; Herbert, A.; Rich, A.; Oschkinat, H. *Proc. Natl. Acad. Sci. U.S.A.* **1999**, *96*, 12465–12470.

- (10) Herbert, A. G.; Rich, A. *Nucleic Acids Res.* **1993**, *21*, 2669–2672.

- (11) Herbert, A.; Alfken, J.; Kim, Y. G.; Mian, I. S.; Nishikura, K.; Rich, A. *Proc. Natl. Acad. Sci. U.S.A.* **1997**, *94*, 8421–8426.

- (12) Herbert, A.; Schade, M.; Lowenhaupt, K.; Alfken, J.; Schwartz, T.; Shlyakhtenko, L. S.; Lyubchenko, Y. L.; Rich, A. *Nucleic Acids Res.* **1998**, *26*, 3486–3493.

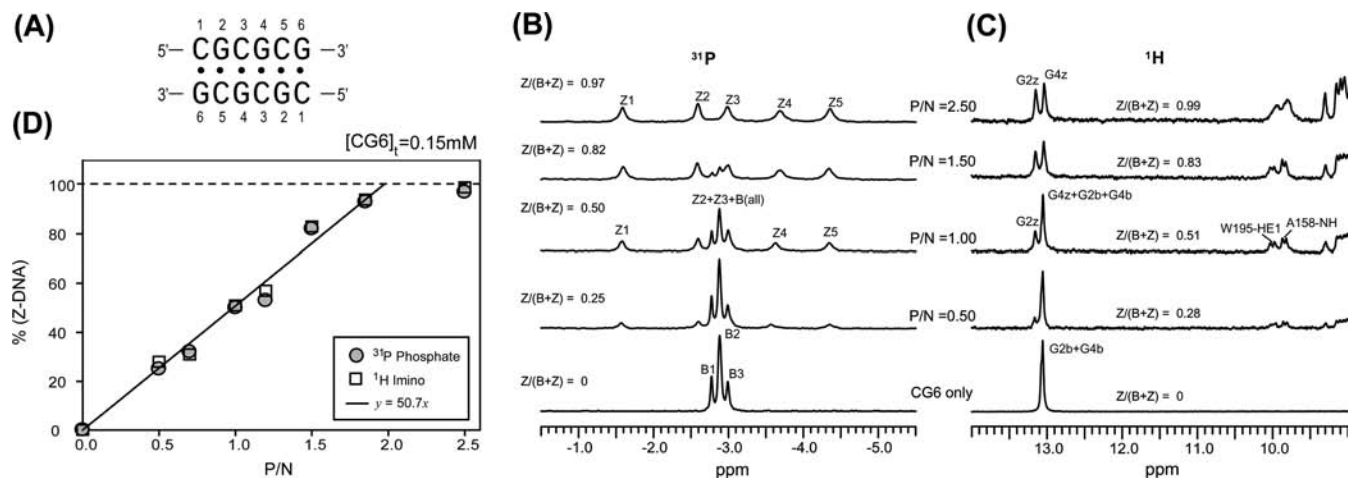


**Figure 1.** (A) Sequence context of the CG6 duplex and (B) <sup>31</sup>P NMR and (C) imino proton spectra of the CG6 substrate at 35 °C upon titration with Z $\alpha$ <sub>ADAR1</sub>. In the <sup>31</sup>P spectra, three resonances from B-form and five resonances from Z-DNA were denoted as B1–B3 and Z1–Z5, respectively. In the imino proton spectra, the resonances from B-form were denoted as G2b and G4b and those from Z-form were denoted as G2z and G4z. P/N ratios are shown in the middle of the two spectra. (D) Percent of CG6 molecules in the Z-conformation within the total CG6 population as a function of P/N ratio, determined by relative peak intensities of the Z-DNA resonances in the <sup>31</sup>P (gray circles) and imino proton (open squares) spectra. A straight solid line is the best fit to a linear correlation between Z-DNA population and the P/N ratio.

that one monomeric Z $\alpha$  domain binds to one strand of double-stranded Z-DNA, while a second monomer binds to the opposite strand, yielding 2-fold symmetry with respect to the DNA helical axis.<sup>6</sup> Z $\alpha$ <sub>ADAR1</sub> shares high structural similarity to ( $\alpha + \beta$ ) helix–turn–helix B-DNA binding proteins but binds preferentially to Z-DNA, rather than B-DNA, with high affinity [ $K_d = 30$  nM for d(CGCGCG)<sub>2</sub>].<sup>9</sup> Structural studies of Z $\alpha$  domains from species other than human by X-ray crystallography or NMR spectroscopy have suggested that a few different structural differences found among them might be related to their Z-DNA binding affinity and functions in the cell, even though their overall structures are very similar to each other.<sup>13–15</sup> It has been suggested that the specificity of Z $\alpha$ <sub>ADAR1</sub> binding to left-handed Z-DNA results from two structural properties: (i) binding of Z $\alpha$ <sub>ADAR1</sub> to B-DNA is not favored because of steric hindrance, and (ii) binding of Z $\alpha$ <sub>ADAR1</sub> to Z-DNA is favored because of contributions from electrostatic contact between the phosphate backbone of Z-DNA and the side chain of Z $\alpha$ <sub>ADAR1</sub>.<sup>9</sup> Although these structural studies explain well the specificities of Z $\alpha$  family proteins for Z-DNA, the detailed molecular mechanism by which Z $\alpha$  proteins converts a right-handed backbone structure in a substrate DNA duplex to a left-handed Z-form is not well understood.

Here, we have performed CD and NMR experiments on complexes between Z $\alpha$ <sub>ADAR1</sub> and the 6-bp DNA duplex d(CGCGCG)<sub>2</sub> (referred to as CG6, Figure 1A) produced with a variety of protein-to-DNA (P/N) molar ratios. The hydrogen exchange rate constants ( $k_{ex}$ ) for the imino protons in the complexes were determined as a function of P/N ratios by NMR spectroscopy. This approach allows detection of the intermediate states of the CG6–Z $\alpha$ <sub>ADAR1</sub> complex and provides the informa-

tion required to identify how the Z $\alpha$ <sub>ADAR1</sub>-induced B–Z conformational change occurs in a DNA double helix.

## Experimental Section

**Sample Preparation.** The DNA oligomer d(CGCGCG) was purchased from M-biotech Inc. (Seoul, Korea). This DNA oligomer was purified by reverse-phase HPLC and desalted on a Sephadex G-25 gel-filtration column. DNA duplex samples (CG6) were dissolved in a 90% H<sub>2</sub>O/10% D<sub>2</sub>O NMR buffer that contained 10 mM sodium phosphate (pH 8.0) and 100 mM NaCl. The amount of CG6 was represented as the concentration of the double-stranded sample, which was half that of d(CGCGCG). To produce <sup>15</sup>N-labeled or <sup>13</sup>C,<sup>15</sup>N-labeled Z $\alpha$ <sub>ADAR1</sub>, BL21(DE3) bacteria were grown in M9 medium that contained 1 g/L <sup>15</sup>NH<sub>4</sub>Cl and/or 2 g/L <sup>13</sup>C-glucose. Expression and purification of <sup>15</sup>N-labeled or <sup>13</sup>C,<sup>15</sup>N-labeled Z $\alpha$ <sub>ADAR1</sub> has been described in a previous report.<sup>16</sup> The protein concentration was measured spectroscopically by use of an extinction coefficient of 6970 M<sup>-1</sup> cm<sup>-1</sup> at 280 nm. The protein samples were dissolved in a 90% H<sub>2</sub>O/10% D<sub>2</sub>O NMR buffer that contained 10 mM sodium phosphate (pH 8.0) and 100 mM NaCl.

**NMR Experiments.** All <sup>1</sup>H, <sup>13</sup>C, and <sup>15</sup>N NMR experiments were performed on a Varian Inova 600 MHz spectrometer (KAIST, Daejeon) equipped with a triple-resonance probe or a 900 MHz spectrometer (KIST, Seoul) equipped with a cold probe. The <sup>31</sup>P NMR experiments were performed on a Varian 500 MHz spectrometer (Varian Technologies, Seoul) equipped with a broadband probe. All three-dimensional (3D) triple resonance experiments and 2D nuclear Overhauser effect spectroscopy (NOESY) experiments were carried out with 1 mM <sup>13</sup>C,<sup>15</sup>N-labeled Z $\alpha$ <sub>ADAR1</sub> in the free or CG6-complexed forms (at a P/N ratio of 1 or 2). The 1D <sup>1</sup>H and <sup>31</sup>P NMR spectra were obtained from complex samples that were prepared by addition of <sup>15</sup>N-labeled Z $\alpha$ <sub>ADAR1</sub> to 0.15 mM CG6 in an NMR buffer at the indicated P/N ratio. One-dimensional data were processed with the program FELIX2004 (Accelrys, San Diego, CA). Two- and three-dimensional data were processed with the program NMRPIPE<sup>17</sup> and analyzed by the program SPARKY.<sup>18</sup> External 2,2-dimethyl-2-silapentane-5-sulfonate was used for the

(13) Schwartz, T.; Behlke, J.; Lowenhaupt, K.; Heinemann, U.; Rich, A. *Nat. Struct. Biol.* **2001**, *8*, 761–765.

(14) Kahmann, J. D.; Wecking, D. A.; Putter, V.; Lowenhaupt, K.; Kim, Y. G.; Schmieder, P.; Oschkinat, H.; Rich, A.; Schade, M. *Proc. Natl. Acad. Sci. U.S.A.* **2004**, *101*, 2712–2717.

(15) Ha, S. C.; Lokanath, N. K.; Van Quyen, D.; Wu, C. A.; Lowenhaupt, K.; Rich, A.; Kim, Y. G.; Kim, K. K. *Proc. Natl. Acad. Sci. U.S.A.* **2004**, *101*, 14367–14372.

(16) Ha, S. C.; Lowenhaupt, K.; Rich, A.; Kim, Y. G.; Kim, K. K. *Nature* **2005**, *437*, 1183–1186.

(17) Delaglio, F.; Grzesiek, S.; Vuister, G. W.; Zhu, G.; Pfeifer, J.; Bax, A. *J. Biomol. NMR* **1995**, *6*, 277–293.

(18) Goddard, T. D.; Kneller, D. G. SPARKY; University of California, San Francisco, 2003.

$^1\text{H}$ ,  $^{13}\text{C}$ , and  $^{15}\text{N}$  references, and sodium phosphate was used as the  $^{31}\text{P}$  reference.

$^1\text{H}$ ,  $^{13}\text{C}$ , and  $^{15}\text{N}$  backbone resonance assignments for free  $\text{Z}\alpha_{\text{ADAR1}}$  and the  $\text{CG6}-\text{Z}\alpha_{\text{ADAR1}}$  complexes were obtained from the following 3D experiments: CBCA(CO)NH, HNCACB, HNCO, HNCA, HCCH–TOCSY, NOESY– $^1\text{H}/^{15}\text{N}$ -HSQC, and NOESY– $^1\text{H}/^{13}\text{C}$ -HSQC (HSQC = heteronuclear single quantum coherence; TOCSY = total correlation spectroscopy). The imino proton resonance assignments for free CG6 and the  $\text{CG6}-\text{Z}\alpha_{\text{ADAR1}}$  complexes were obtained from 2D Watergate NOESY and  $^{13}\text{C},^{15}\text{N}$ -filtered NOESY spectra, respectively. The average chemical shift differences of the amide proton and nitrogen resonances between the free  $\text{Z}\alpha_{\text{ADAR1}}$  and  $\text{Z}\alpha_{\text{ADAR1}}$  in complex with CG6 were calculated by using eq 1:

$$\Delta\delta_{\text{avg}} = \sqrt{(\Delta\delta_{\text{H}})^2 + (\Delta\delta_{\text{N}}/5.88)^2} \quad (1)$$

where  $\Delta\delta_{\text{H}}$  and  $\Delta\delta_{\text{N}}$  are the chemical shift differences of the amide proton and nitrogen resonances, respectively.

Diffusion coefficients of free  $\text{Z}\alpha_{\text{ADAR1}}$  and the  $\text{CG6}-\text{Z}\alpha_{\text{ADAR1}}$  complexes at P/N = 1.0 and 2.0 were determined by a modified pulsed gradient spin–echo experiment.<sup>19</sup> The intensities of resonances were measured with different gradients varying in amplitude from 1 to 35 G/cm.

**Hydrogen Exchange Rate Measurement.** The apparent longitudinal relaxation rate constants ( $R_{1a} = 1/T_{1a}$ ) of the imino protons of free CG6 and the  $\text{CG6}-\text{Z}\alpha_{\text{ADAR1}}$  complexes at various P/N ratios were determined by semiselective inversion recovery 1D NMR experiments. The apparent relaxation rate constant of water ( $R_{1w}$ ) was determined by a selective inversion recovery experiment, using a DANTE sequence for selective water inversion.<sup>20</sup>  $R_{1a}$  and  $R_{1w}$  were determined by curve fitting of the inversion recovery data to the appropriate single-exponential function. The hydrogen exchange rate constants ( $k_{\text{ex}}$ ) of the imino protons were measured by a water magnetization transfer experiment. The intensities of each imino proton were measured with 20 different delay times. The  $k_{\text{ex}}$  values for the imino protons were determined by fitting the data to eq 2:

$$\frac{I_0 - I(t)}{I_0} = 2 \frac{k_{\text{ex}}}{(R_{1w} - R_{1a})} (e^{-R_{1a}t} - e^{-R_{1w}t}) \quad (2)$$

where  $I_0$  and  $I(t)$  are the peak intensities of the imino proton in the water magnetization transfer experiments at times 0 and  $t$ , respectively, and  $R_{1a}$  and  $R_{1w}$  are the apparent longitudinal relaxation rate constants for the imino proton and water, respectively, measured in semiselective inversion recovery 1D NMR experiments.<sup>20,21</sup>

**CD Experiments.** CD spectra for free CG6 and  $\text{CG6}-\text{Z}\alpha_{\text{ADAR1}}$  complexes at various P/N ratios were obtained at 25 °C, on a Jasco J-815 spectrometer. The NMR samples—in which the total concentration of CG6 was 0.15 mM, as indicated by the P/N ratio above—were diluted and used in the CD experiments.

**Gel-Filtration Chromatography Experiments.** Gel-filtration chromatography experiments for  $\text{CG6}-\text{Z}\alpha_{\text{ADAR1}}$  complexes with the P/N ratios of 1.0, 1.5, or 1.85 were performed on a Sephacryl S-100 HR column (GE Healthcare Inc.) on a GE AKTA Prime Plus. NMR samples (20  $\mu\text{L}$ ), in which the total concentration of CG6 was 0.15 mM, were injected directly into the column.

## Results

**Titration of  $\text{Z}\alpha_{\text{ADAR1}}$  to CG6.** Two-dimensional NOESY spectra were used to assign the imino proton resonances of the CG6 DNA duplex. Figure 1C shows the titration of CG6 with  $\text{Z}\alpha_{\text{ADAR1}}$ , where the 1D imino proton spectra change until the P/N ratio reaches 2 and no free CG6 is observed. Further

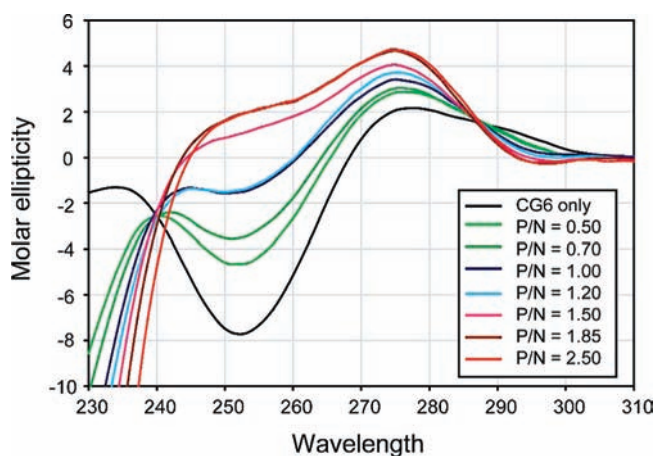


**Figure 2.** Conversion of B-form to Z-form of CG6 upon titration with  $\text{Z}\alpha_{\text{ADAR1}}$ , measured by CD in the range 230–310 nm.

addition of  $\text{Z}\alpha_{\text{ADAR1}}$  up to P/N = 2.5 resulted in no changes in the imino proton spectrum. Formation of the  $\text{CG6}-\text{Z}\alpha_{\text{ADAR1}}$  complex was also monitored by 2D  $^1\text{H}/^{15}\text{N}$ -HSQC spectra. Both 1D imino and 2D HSQC spectra exhibited slow exchange of the NMR resonance, as expected for a tight binding complex.  $^{31}\text{P}$  chemical shifts are a sensitive probe of backbone conformational change of oligonucleotides and are especially valuable for studying nucleic acid–protein interactions.<sup>22,23</sup> Figure 1B shows the change of  $^{31}\text{P}$  NMR spectra of the CG6 substrate upon addition of  $\text{Z}\alpha_{\text{ADAR1}}$ . There is a striking change in the  $^{31}\text{P}$  NMR spectrum of CG6 when bound to  $\text{Z}\alpha_{\text{ADAR1}}$ , with five resonances dispersed over 3 ppm. This  $^{31}\text{P}$  fingerprint is therefore diagnostic of the  $\text{CG6}-\text{Z}\alpha_{\text{ADAR1}}$  interaction.

The B–Z transition of the CG6 substrate upon addition of  $\text{Z}\alpha_{\text{ADAR1}}$  was confirmed by CD spectra, in which large alterations of the molar ellipticity were observed at 255 and 295 nm (Figure 2). The less negative peak at 295 nm means that the left-handed conformation induced by  $\text{Z}\alpha_{\text{ADAR1}}$  differs slightly from the  $\text{Mg}^{2+}$ -stabilized Z-DNA.<sup>11</sup> Thus new resonances in the  $^{31}\text{P}$  NMR ( $\text{Z1}\sim\text{Z5}$ ) and imino proton spectra ( $\text{G2z}$  and  $\text{G4z}$ ) at 35 °C are indicative of left-handed Z-form helix generation in the CG6 induced by  $\text{Z}\alpha_{\text{ADAR1}}$  (Figure 1B,C). Figure 1D shows the relative populations of Z-DNA, which were determined by the integration of new resonances ( $\text{Z1}\sim\text{Z5}$ ,  $\text{G2z}$ , and  $\text{G4z}$ ) as a function of the P/N ratio. Surprisingly, Z-DNA was produced as half the total amount ( $P_t$ ) of added  $\text{Z}\alpha_{\text{ADAR1}}$  until the P/N ratio was up to 2 ( $Z_t = 1/2P_t$ ); then, when  $P/N \geq 2$ , 100% of the CG6 substrate exhibited the Z-conformation (Figure 1D).

**Chemical Shift Change of  $\text{Z}\alpha_{\text{ADAR1}}$  upon Binding to CG6.** A superposition of the  $^1\text{H}/^{15}\text{N}$ -HSQC spectra of free  $\text{Z}\alpha_{\text{ADAR1}}$  and  $\text{Z}\alpha_{\text{ADAR1}}$  bound to CG6 (P/N ratio = 2) is shown in Figure 3A. Amide backbone resonance assignments for free  $\text{Z}\alpha_{\text{ADAR1}}$  and  $\text{Z}\alpha_{\text{ADAR1}}-\text{CG6}$  complex were made by heteronuclear NMR experiments [NOESY– $^1\text{H}/^{15}\text{N}$ -HSQC, HNCACB, and CACB-(CO)NH]. In the  $^1\text{H}/^{15}\text{N}$ -HSQC spectrum of the  $\text{Z}\alpha_{\text{ADAR1}}-\text{CG6}$  complex, all the amide backbone cross peaks of the residues E140~Q202 were assigned (Figure 3). The secondary structure of  $\text{Z}\alpha_{\text{ADAR1}}$  in the complex with CG6 substrate was assessed from sequential and medium-range NH–NH and NH–H $\alpha$  NOE patterns in the NOESY– $^1\text{H}/^{15}\text{N}$ -HSQC spectra (data not shown).

(19) Nesselova, I. V.; Idiyatullin, D.; Mayo, K. H. *J. Magn. Reson.* **2004**, *166*, 129–133.

(20) Lee, J.-H.; Pardi, A. *Nucleic Acids Res.* **2007**, *35*, 2965–2974.

(21) Lee, J.-H.; Jucker, F.; Pardi, A. *FEBS Lett.* **2008**, *582*, 1835–1839.

(22) Gorenstein, D. G. *Phosphorus-31 NMR: Principles and Applications*; Academic Press: Orlando, FL, 1984.

(23) Castagne, C.; Murphy, E. C.; Gronenborn, A. M.; Delepierre, M. *Eur. J. Biochem.* **2000**, *267*, 1223–1229.

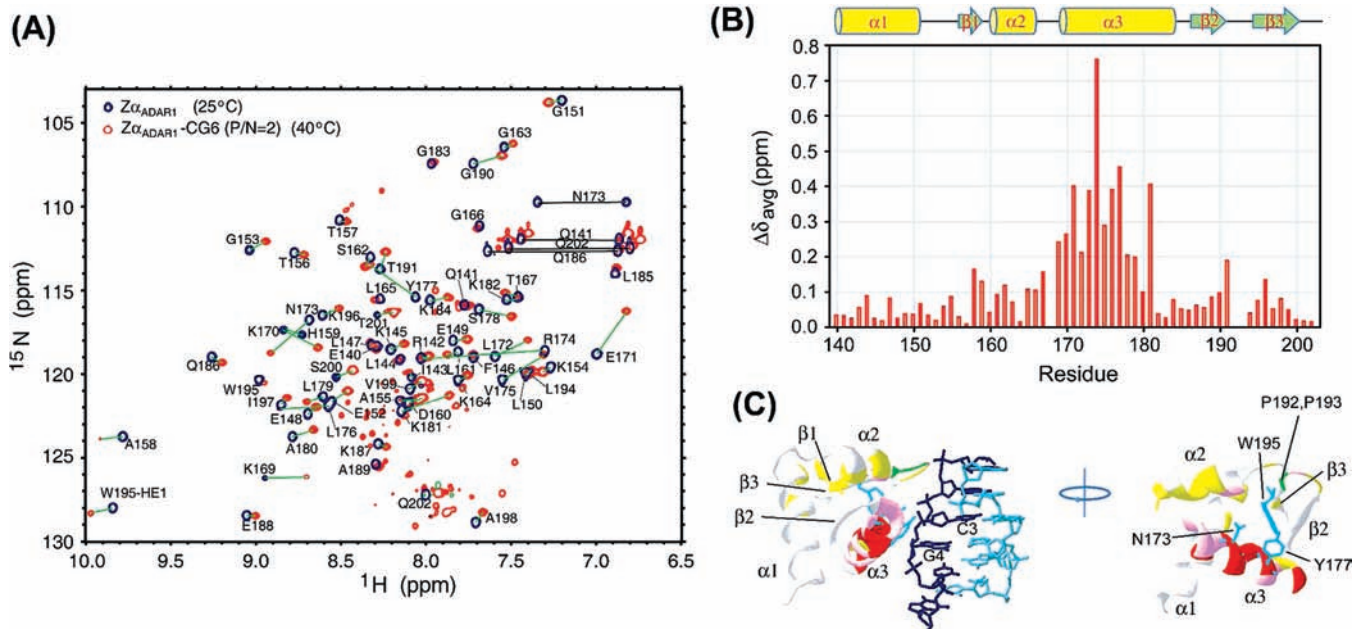


**Figure 3.** (A) Superposition of  $^1\text{H}/^{15}\text{N}$ -HSQC spectra of free  $Z\alpha_{\text{ADAR1}}$  at  $25^\circ\text{C}$  (blue) and  $Z\alpha_{\text{ADAR1}}-\text{CG6}$  complex (P/N ratio = 2) at  $40^\circ\text{C}$  (red). Green solid lines indicate cross-peak movements by binding of  $Z\alpha_{\text{ADAR1}}$  to CG6. Black solid lines indicate the amide signals of side chains of Asn (N) and Gln (Q) residues. (B) Red bars are the weighted average  $^1\text{H}/^{15}\text{N}$  chemical shift changes ( $\Delta\delta_{\text{avg}}$ ) of the  $Z\alpha_{\text{ADAR1}}$  upon binding to CG6 (P/N = 2) at  $40^\circ\text{C}$ . When amide resonances of some residues were not observed in the spectrum of free  $Z\alpha_{\text{ADAR1}}$  at  $40^\circ\text{C}$ , chemical shift values at  $25^\circ\text{C}$  were used in this calculation. (C) Secondary structure model for previously determined X-ray crystal structure of the  $Z\alpha_{\text{ADAR1}}$  bound to Z-DNA (PDB id = 1QBJ). Colors used to illustrate  $^1\text{H}/^{15}\text{N}$  chemical shift changes upon CG6 binding are red,  $>0.3$  ppm; magenta,  $0.15\text{--}0.3$  ppm; and yellow,  $0.08\text{--}0.15$  ppm.

The  $\alpha 1\text{--}\beta 1\text{--}\alpha 2\text{--}\alpha 3\text{--}\beta 2\text{--}\beta 3$  secondary structure of the  $Z\alpha_{\text{ADAR1}}$  is basically unchanged in the complex in solution, allowing the use of chemical shift mapping to probe the DNA binding site.

The weighted average  $^1\text{H}/^{15}\text{N}$  backbone chemical shift changes were determined for each residue by using eq 1 (Figure 3B). All residues of the  $\alpha 3$  helix underwent chemical shift changes larger than  $0.1$  ppm upon binding to the CG6 substrate (Figure 3B). Residues E171, N173, R174, L176, Y177, and K181 represent the significant backbone chemical shift changes larger than  $0.3$  ppm (Figure 3). In addition, significant chemical shift changes were observed in the  $\beta 1\text{--}\alpha 2$  and  $\beta 2\text{--loop--}\beta 3$  regions (Figure 3). These results indicate the direct interaction of their side chains with the phosphate backbone of the CG6 substrate as reported in the previous crystal structural study.<sup>6</sup>

Except for the amide signal from H159, the  $^1\text{H}/^{15}\text{N}$ -HSQC spectrum of  $Z\alpha_{\text{ADAR1}}-\text{CG6}$  complex at P/N = 1 was well superimposed with that obtained at P/N = 2, which indicates the  $\text{CG6}-(Z\alpha_{\text{ADAR1}})_2$  complex (Figure 4A). Figure 4B,C shows the  $T_1$  relaxation times and  $^1\text{H}/^{15}\text{N}$  heteronuclear NOEs at  $35^\circ\text{C}$  for each residue of the complexes at P/N = 1 and 2. Interestingly, the dynamics properties of the amide backbone of the  $Z\alpha_{\text{ADAR1}}-\text{CG6}$  complex at P/N = 1 and 2 significantly contrast with each other (Figure 4B,C). This comparison revealed that the conformational state of  $Z\alpha_{\text{ADAR1}}$  in the complex formed at P/N = 1 is not the  $\text{CG6}-(Z\alpha_{\text{ADAR1}})_2$  complex but may be a mixture of the various conformational states such as  $\text{CG6}-Z\alpha_{\text{ADAR1}}$  and  $\text{CG6}-(Z\alpha_{\text{ADAR1}})_2$ . The existence of these complexes in the complete complex population at P/N = 1 was confirmed by the significant line broadening of the resonances in the  $^{31}\text{P}$  NMR spectra assigned to the B-form (Supporting Information, Figure S1). The diffusion coefficients of free  $Z\alpha_{\text{ADAR1}}$  and of  $\text{CG6}-Z\alpha_{\text{ADAR1}}$  complexes at P/N = 1.0 and 2.0 determined at  $35^\circ\text{C}$  by a modified pulsed gradient spin-echo experiment<sup>19</sup> are  $(1.29 \pm 0.01) \times 10^{-6}$ ,  $(0.92 \pm 0.03) \times 10^{-6}$ , and  $(0.79 \pm 0.01) \times 10^{-6}$   $\text{cm}^2/\text{s}$ , respectively (Sup-

porting Information, Figure S2). These results strongly supported that the complex state at P/N = 1.0 had a larger molecular weight than free  $Z\alpha_{\text{ADAR1}}$  but smaller than the  $\text{CG6}-(Z\alpha_{\text{ADAR1}})_2$  complex. Thus we could suggest that the major complex state at P/N = 1.0 has a 1:1 molar ratio between CG6 and  $Z\alpha_{\text{ADAR1}}$ . This hypothesis is also supported by the observation of two peaks in the Gel-filtration chromatography profiles of the  $\text{CG6}-Z\alpha_{\text{ADAR1}}$  complexes at P/N = 1.0, 1.5, and 1.85 (Figure 5).

**Exchange Rate Constants of G2z Imino Protons.** The  $k_{\text{ex}}$  values of the imino protons in free CG6 and  $\text{CG6}-Z\alpha_{\text{ADAR1}}$  complexes at various P/N ratios were determined at  $35^\circ\text{C}$  by the water magnetization transfer method (Figure 6).<sup>20,21,24</sup> The G2b and G4b imino protons of free CG6 have  $k_{\text{ex}}$  values of  $20.7 \pm 0.2$  and  $12.0 \pm 0.2$   $\text{s}^{-1}$ , respectively. The G2z ( $k_{\text{ex}} = 4.8 \pm 0.9$   $\text{s}^{-1}$ ) and G4z ( $k_{\text{ex}} = 0.8 \pm 0.8$   $\text{s}^{-1}$ ) imino protons of the Z-form at P/N = 2.5 were more slowly exchanged than those of the B-form (Figure 6B). Figure 6C shows  $k_{\text{ex}}$  data for the G2z imino proton, where  $k_{\text{ex}}$  decreased from 11.1 to 4.8  $\text{s}^{-1}$  as the P/N ratio increased from 0.7 to 2.5. This observation might be explained by the possible presence of a mixture of two G2 imino resonances from the  $\text{CG6}-Z\alpha_{\text{ADAR1}}$  and  $\text{CG6}-(Z\alpha_{\text{ADAR1}})_2$  complexes in the G2z peak. Thus the observed  $k_{\text{ex}}$  for the G2z imino proton is given by

$$k_{\text{ex}} = \frac{[\text{ZP}]k_{\text{ex}}^{\text{ZP}} + [\text{ZP}_2]k_{\text{ex}}^{\text{ZP}_2}}{[\text{ZP}] + [\text{ZP}_2]} \quad (3)$$

where  $[\text{ZP}]$  and  $[\text{ZP}_2]$  are the concentrations of the  $\text{CG6}-Z\alpha_{\text{ADAR1}}$  and  $\text{CG6}-(Z\alpha_{\text{ADAR1}})_2$  complexes, respectively, and  $k_{\text{ex}}^{\text{ZP}}$  and  $k_{\text{ex}}^{\text{ZP}_2}$  are the exchange rate constants of G2z imino protons

(24) Gueron, M.; Leroy, J. L. *Methods Enzymol.* **1995**, *261*, 383–413.

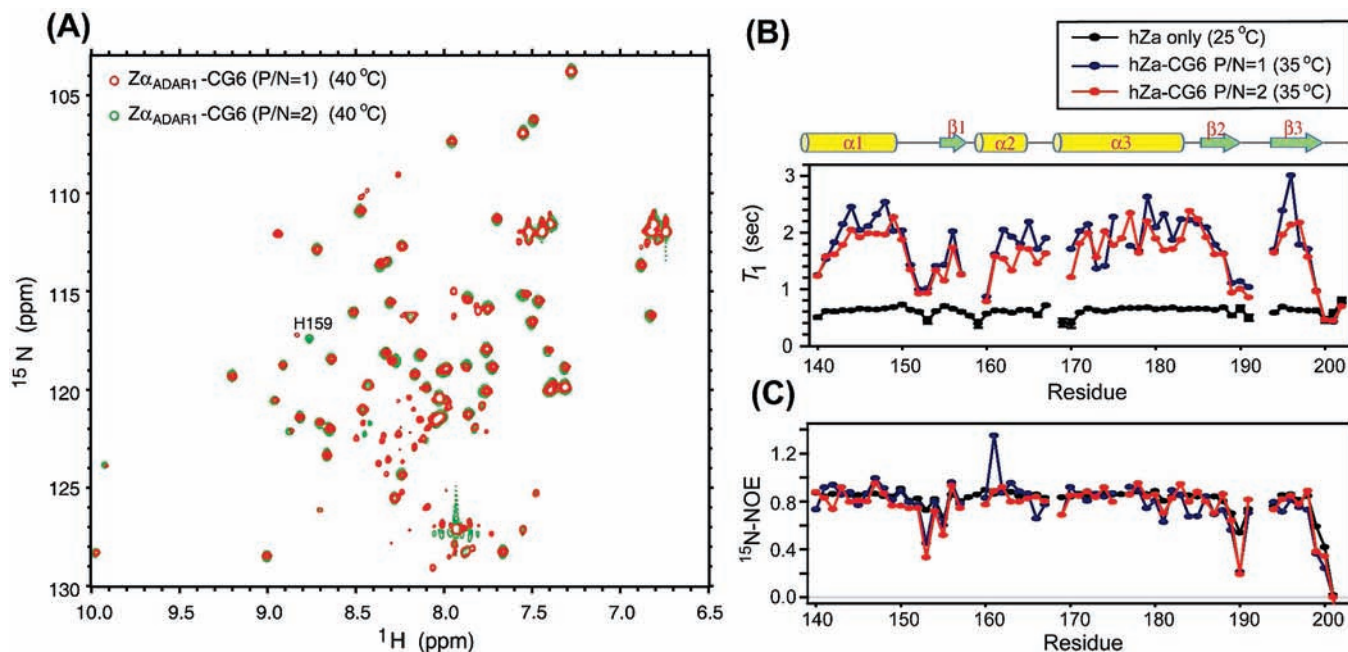


**Figure 4.** (A) Superposition of  $^1\text{H}/^{15}\text{N}$ -HSQC spectra of the  $Z\alpha$ -CG6 complexes at P/N = 1 (red) and P/N = 2 (green) at 40 °C. (B)  $T_1$  relaxation times and (C)  $^{15}\text{N}/^1\text{H}$  heteronuclear NOE of the amide signals of free  $Z\alpha_{\text{ADAR1}}$  at 25 °C (black) and  $Z\alpha_{\text{ADAR1}}$ -CG6 complex at P/N = 1 (blue) and P/N = 2 (red) at 35 °C. Positions of secondary structure elements are shown for the  $Z\alpha_{\text{ADAR1}}$ -DNA complex.<sup>6</sup>

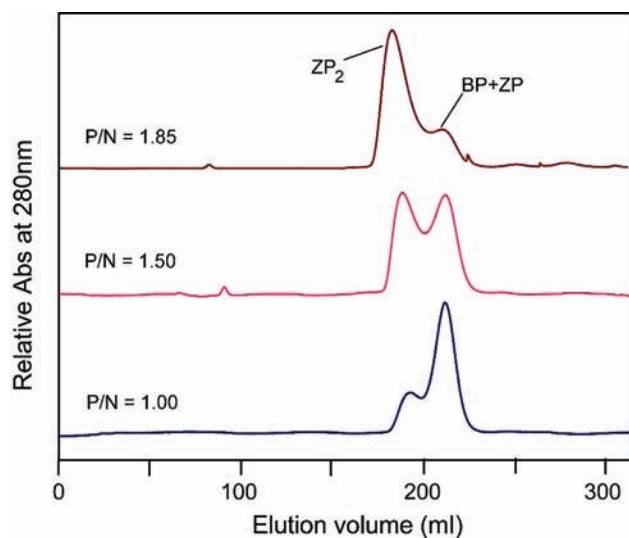


**Figure 5.** Gel-filtration chromatography profiles of CG6- $Z\alpha_{\text{ADAR1}}$  complexes at P/N = 1.0 (blue), 1.5 (magenta), and 1.85 (brown) monitored at 280 nm. The column volume is 320 mL.

for the CG6- $Z\alpha_{\text{ADAR1}}$  and CG6-( $Z\alpha_{\text{ADAR1}}$ )<sub>2</sub> complexes, respectively.

## Discussion

In the absence of direct experimental evidence that elucidates when the conformational change from B-DNA to Z-DNA occurs during complex formation between  $Z\alpha_{\text{ADAR1}}$  and a 6-base-pair (bp) DNA substrate, two general mechanisms, termed *passive* and *active*, have been put forward (Figure 7). The passive B–Z transition mechanism envisions that  $Z\alpha_{\text{ADAR1}}$  (denoted as **P**) binds directly to the DNA when its B-form (denoted as **B**) is changed to a Z-form (denoted as **Z**), and the **ZP** complex is created. The active mechanism has two possible pathways

depending on the number of  $Z\alpha_{\text{ADAR1}}$  molecules involved in the B–Z transition: (i) *active-mono* B–Z conversion, in which one molecule of **P** binds to **B** to form a **BP** complex and the conformational transition from **BP** to **ZP** follows, or (ii) *active-di* B–Z conversion, in which two **P** and one **B** form a **BP**<sub>2</sub> complex, which then converts to a **ZP**<sub>2</sub> complex. Recently, imino proton exchange studies successfully proved the molecular mechanism of the enzymatic search for a damaged base in a DNA duplex.<sup>25–27</sup> Similarly, this study provides relevant data to evaluate the energetic feasibility of the active and passive mechanisms for the B–Z transition in a 6-bp DNA by  $Z\alpha_{\text{ADAR1}}$  (Figure 7).

The CG6 substrate exhibits only B-form under  $[\text{NaCl}] \leq 1$  M, but the Z-form begins to appear when  $[\text{NaCl}] \geq 2$  M (Supporting Information, Figure S3). These results mean that  $K_{\text{BZ}}^0 (= [\text{Z}]/[\text{B}])$  is much smaller than 1, indicating that the transition from **B** to **Z** does not occur under physiological conditions. Therefore, it is unlikely that **ZP** is formed by the direct binding of **P** to **Z**.

The 1D imino proton and  $^{31}\text{P}$  NMR study on the formation of the CG6- $Z\alpha_{\text{ADAR1}}$  complex revealed that 100% of the CG6 substrate exhibited the Z-conformation when P/N  $\geq 2$  (Figure 1). This phenomenon was confirmed by CD spectra of the CG6 substrate upon addition of  $Z\alpha_{\text{ADAR1}}$  (Figure 2). These results indicate that  $K_{\text{BZ}}^2 (= [\text{ZP}_2]/[\text{BP}_2])$  is much larger than 1. As a result, the **BP**<sub>2</sub> complex could not be observed as an intermediate structure in this study.

This study revealed that Z-DNA was produced as half the total amount ( $P_1$ ) of the added  $Z\alpha_{\text{ADAR1}}$  when the P/N ratio was less than 2 ( $Z_1 = \frac{1}{2}P_1$ ) (Figure 1). In addition, the  $^1\text{H}/^{15}\text{N}$ -HSQC

(25) Cao, C.; Jiang, Y. L.; Stivers, J. T.; Song, F. *Nat. Struct. Mol. Biol.* **2004**, *11*, 1230–1236.

(26) Cao, C.; Jiang, Y. L.; Krosky, D. J.; Stivers, J. T. *J. Am. Chem. Soc.* **2006**, *128*, 13034–13035.

(27) Parker, J. B.; Bianchet, M. A.; Krosky, D. J.; Friedman, J. I.; Amzel, L. M.; Stivers, J. T. *Nature* **2007**, *449*, 433–437.

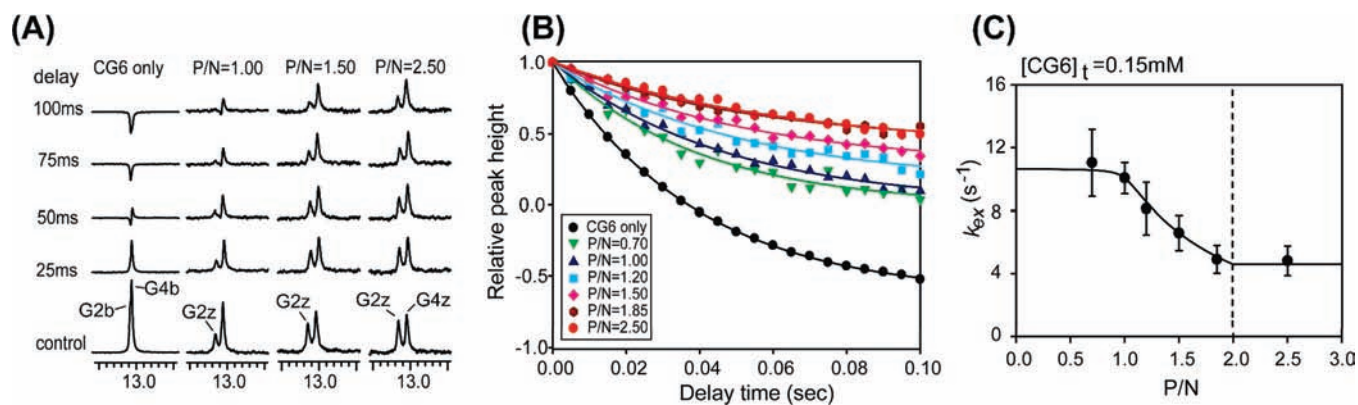


**Figure 6.** (A) One-dimensional imino proton spectra of the water magnetization transfer experiments for free CG6 and CG6–Z $\alpha$ <sub>ADAR1</sub> complexes at P/N = 1.0, 1.5, and 2.5 at 35 °C. (B) Relative peak intensities in the water magnetization transfer spectra for G2z imino resonances of the CG6–Z $\alpha$ <sub>ADAR1</sub> complexes of various P/N ratios as a function of delay time after water inversion. Peak intensities for the G2b imino resonance of free CG6 are also shown as control data. Solid lines are the best fit to eq 2. (C) Exchange rate constants of the G2z imino protons for the CG6–Z $\alpha$ <sub>ADAR1</sub> complexes at 35 °C as a function of P/N ratio. Solid line is the best fit to eq 5 where the  $k_{\text{ex}}$  data points were weighted by the inverse of their variance. Error bars represent curve fitting errors during the determination of  $k_{\text{ex}}$  from water magnetization transfer data.

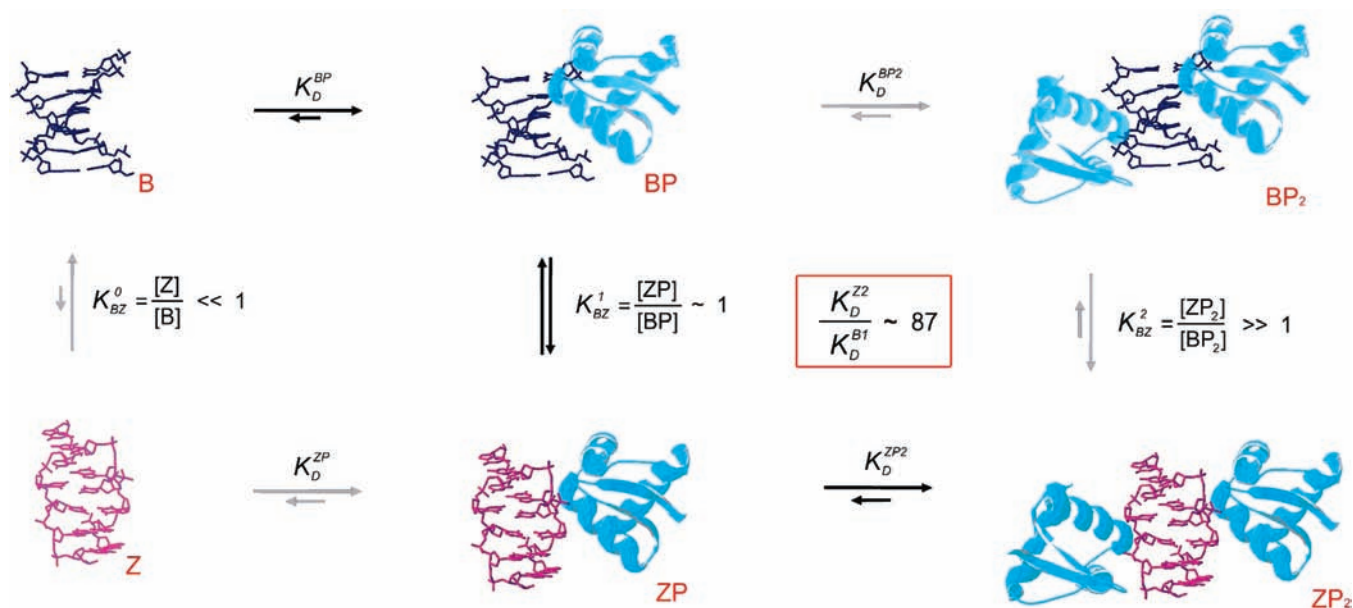


**Figure 7.** Mechanisms for the B–Z conformational transition of a 6-bp DNA duplex by two Z $\alpha$ <sub>ADAR1</sub> proteins.

spectrum of the Z $\alpha$ <sub>ADAR1</sub>–CG6 complex at P/N = 1 was well superimposed with that obtained at P/N = 2 (Figure 4A). These two findings could suggest a hypothesis that two molecules of Z $\alpha$ <sub>ADAR1</sub> (**P**) bind to the DNA and form a **ZP**<sub>2</sub> complex; the remaining DNA substrates exist as B-form (**B**). According to this hypothesis, the backbone dynamics of Z $\alpha$ <sub>ADAR1</sub> and hydrogen exchange pattern of the imino proton of the Z-DNA should be uniform in all complex states. However, this study found two interesting things, which contradict the above hypothesis: (i)  $k_{\text{ex}}$  of the G2z imino proton decreased as the P/N ratio was increased up to 2 (Figure 6), and (ii)  $T_1$  relaxation times and <sup>1</sup>H/<sup>15</sup>N heteronuclear NOEs for each residue of the complexes at P/N = 1 and 2 significantly contrast with each other (Figure 4). Thus, the new hypothesis, in which the **BP** and/or **ZP** complexes exist as intermediate structures, is required.

On the basis of the new hypothesis, the results shown in Figures 1D and 6 yield eq 4, as described in detail in the Supporting Information:

$$[\text{ZP}] \approx [\text{BP}] \quad (4)$$

where  $[\text{ZP}]$  and  $[\text{BP}]$  are the concentrations of the **ZP** and **BP** complexes, respectively. Therefore, the correlation between the observed  $k_{\text{ex}}$  for the G2z imino proton and the P/N ratio is given by eq 5 when P/N ≤ 2:

$$k_{\text{ex}} = k_{\text{ex}}^{\text{ZP}2} + \frac{(k_{\text{ex}}^{\text{ZP}} - k_{\text{ex}}^{\text{ZP}2})}{(1 - \alpha)x} \left\{ 1 - \sqrt{1^2 - 4(1 - \alpha)\left(\frac{x}{2} - \frac{x^2}{4}\right)} \right\} \quad (5)$$

where  $x$  is the P/N ratio and  $\alpha$  ( $=K_D^{\text{BP}}/K_D^{\text{ZP}2}$ ) is the ratio of the dissociation constants of the **BP** and **ZP**<sub>2</sub> complexes (see Supporting Information). The  $\alpha$  value [ $(1.15 \pm 2.69) \times 10^{-2}$ ] and  $k_{\text{ex}}$  values for the G2z protons of **ZP** ( $k_{\text{ex}}^{\text{ZP}} = 10.6 \pm 0.6 \text{ s}^{-1}$ ) and **ZP**<sub>2</sub> ( $k_{\text{ex}}^{\text{ZP}2} = 4.6 \pm 0.2 \text{ s}^{-1}$ ) were determined by curve fitting  $k_{\text{ex}}$  of the G2z protons as a function of P/N ratio with eq 5. When the P/N ratio is larger than 2,  $k_{\text{ex}}$  is kept uniform. This analysis revealed that Z $\alpha$ <sub>ADAR1</sub> (**P**) binds 87-fold more strongly to free CG6 (**B**), to form a **BP** complex, than it does to **ZP** to form a **ZP**<sub>2</sub> complex ( $K_D^{\text{ZP}2}/K_D^{\text{BP}} = 1/\alpha \sim 87$ ).

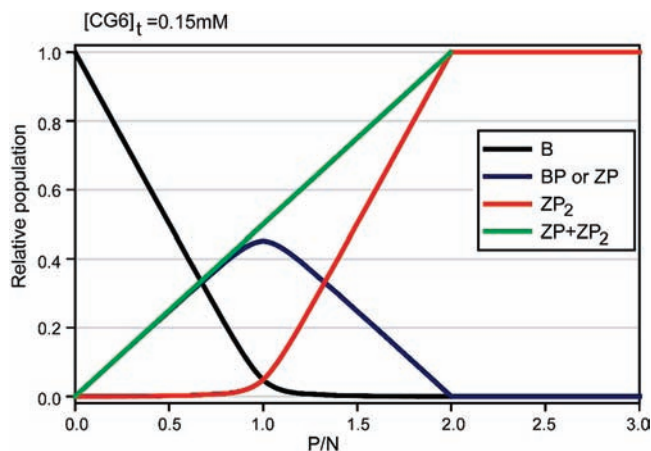


**Figure 8.** Relative populations of the free CG6 [denoted as **B** (black)] and CG6– $Z\alpha_{\text{ADAR1}}$  complexes [**BP**, **ZP** (blue), or **ZP<sub>2</sub>** (red)] as a function of the P/N ratio, which were calculated by eqs 6 and 7. Green line represents the summation of populations of **ZP** and **ZP<sub>2</sub>**.

Relative populations of each complex as a function of P/N ratio could be calculated from eqs 6 and 7, which are described in the Supporting Information in detail (Figure 8):

$$[\text{BP}] = [\text{ZP}] = N_t \left( \frac{1 - \sqrt{1 - 4(1 - \alpha) \left( \frac{x}{2} - \frac{x^2}{4} \right)}}{2(1 - \alpha)} \right) \quad (6)$$

$$[\text{ZP}_2] = N_t \left( \frac{x}{2} - \frac{1 - \sqrt{1 - 4(1 - \alpha) \left( \frac{x}{2} - \frac{x^2}{4} \right)}}{2(1 - \alpha)} \right) \quad (7)$$

where  $x$  is the P/N ratio. That **P** preferentially binds to **B**, rather than other complexes such as **BP** or **ZP**, was confirmed by the observation that [**B**] was gradually decreased, but [**BP**] and [**ZP**] were increased as the P/N ratio increased up to 1 (Figure 8). When the P/N ratio rose to  $\geq 1$ , **ZP** began to bind to the added **P**, producing the **ZP<sub>2</sub>** complex, because free **B** rarely existed under these conditions (Figure 8). This analysis was strongly supported by Gel-filtration chromatography profiles, where the dominant conformation was shown not to be **ZP<sub>2</sub>** but **BP** and/or **ZP** when the P/N ratio is 1.0 (Figure 5).

Our analysis found that the **BP** and **ZP** complexes are the major conformations when the P/N ratio  $\leq 1$ , and the amounts of these two forms are the same and in equilibrium ( $K_{\text{BZ}} = [\text{ZP}]/[\text{BP}] = 1$ ). Conceivably, the addition of a second **P** molecule to **ZP** results in fast shift of the equilibrium toward the Z-conformation of CG6. The existence of both the **BP** and **ZP** conformations strongly supports the active-mono mechanism, in which a single  $Z\alpha_{\text{ADAR1}}$  binds to a 6-bp DNA and then converts its helix to a Z-form, even though the results of this study could not clearly exclude the passive mechanism.

## Conclusions

Human ADAR1 deaminates adenine in pre-mRNA to yield inosine, which codes as guanine.  $Z\alpha_{\text{ADAR1}}$  preferentially binds Z-DNA, rather than B-DNA, with high binding affinity. One monomeric  $Z\alpha_{\text{ADAR1}}$  domain binds to one strand of double-stranded DNA, and a second  $Z\alpha_{\text{ADAR1}}$  monomer binds to the opposite strand with 2-fold symmetry with respect to the DNA helical axis. Here, we have proposed the active mechanism for the B–Z transition of a DNA duplex by  $Z\alpha_{\text{ADAR1}}$  as suggested from the following observations: (i) initially, the  $Z\alpha$  domain (**P**) preferred to bind to B-DNA (**B**) and thus formed **BP**; (ii) simultaneously, the B-form helix of the **BP** complex was converted to left-handed Z-DNA with  $K_{\text{BZ}} = 1$ , and **BP** and **ZP** then existed in equivalent amounts; (iii) finally, the stable **ZP<sub>2</sub>** complex was produced by addition of **P** to a **ZP** population that contained no free **B**.

**Acknowledgment.** This work was supported by the KOSEF Grant (R01-2007-000-10691-0 to J.-H.L.), the KRF Grant (KRF-2008-331-C00178 to J.-H.L.), the National Creative Research Initiative Program (to B.-S.C.), the NRL Program (NRL-2006-02287 to K.K.K.), and the EB-NCRC Grant (R15-2003-012-01001-0) funded by the Korean Government (MEST). We thank the Varian Technologies Korea Inc. and KIST NMR Facility for performing NMR experiments.

**Supporting Information Available:** Details of derivation of equations; figures showing line widths of  $^{31}\text{P}$  NMR spectra as a function of P/N ratio, diffusion decays for free  $Z\alpha_{\text{ADAR1}}$  and CG6– $Z\alpha_{\text{ADAR1}}$  complexes at P/N ratios of 1.0 and 2.0, and NaCl-dependent 1D imino and base proton spectra of the CG6 duplex. This material is available free of charge via the Internet at <http://pubs.acs.org>.

JA902654U